View metadata, citation and similar papers at core.ac.uk

brought to you by CORE

provided by Elsevier - Publisher Connector

Cell Reports
Report

Cell PRESS
Open ACCESS

Homologous Recombination DNA Repair Genes Play a Critical Role in Reprogramming to a Pluripotent State

Federico González,[1] Daniela Georgieva,[1,4] Fabio Vanoli,[1,4] Zhong-Dong Shi,[1] Matthias Stadtfeld,[2] Thomas Ludwig,[3] Maria Jasin,[1,*] and Danwei Huangfu[1,*]

[1]Developmental Biology Program, Sloan-Kettering Institute, 1275 York Avenue, New York, NY 10065, USA

[2]Developmental Genetics Program, Skirball Institute of Biomolecular Medicine, Department of Cell Biology, New York University School of Medicine, 540 1st Avenue, New York, NY 10016, USA

[3]The Ohio State University Wexner Medical Center, The James Comprehensive Cancer Center, 596 Biomedical Research Tower, 460 West 12th Avenue, Columbus, OH 43210, USA

[4]These authors contributed equally to this work

*Correspondence: m-jasin@ski.mskcc.org (M.J.), huangfud@mskcc.org (D.H.)

http://dx.doi.org/10.1016/j.celrep.2013.02.005

SUMMARY

Induced pluripotent stem cells (iPSCs) hold great promise for personalized regenerative medicine. However, recent studies show that iPSC lines carry genetic abnormalities, suggesting that reprogramming may be mutagenic. Here, we show that the ectopic expression of reprogramming factors increases the level of phosphorylated histone H2AX, one of the earliest cellular responses to DNA double-strand breaks (DSBs). Additional mechanistic studies uncover a direct role of the homologous recombination (HR) pathway, a pathway essential for error-free repair of DNA DSBs, in reprogramming. This role is independent of the use of integrative or nonintegrative methods in introducing reprogramming factors, despite the latter being considered a safer approach that circumvents genetic modifications. Finally, deletion of the tumor suppressor *p53* rescues the reprogramming phenotype in HR-deficient cells primarily through the restoration of reprogramming-dependent defects in cell proliferation and apoptosis. These mechanistic insights have important implications for the design of safer approaches to creating iPSCs.

INTRODUCTION

Pioneering work by Yamanaka and colleagues has identified key transcription factors that enable the reprogramming of somatic cells to a pluripotent state (Takahashi and Yamanaka, 2006). This technology has been used to generate human induced pluripotent stem cells (iPSCs), which closely resemble embryonic stem cells (ESCs) in terms of differentiation potential, self-renewal capacity, transcriptional profile, and epigenetic state (Hochedlinger and Plath, 2009; Okita and Yamanaka, 2011). Like ESCs, iPSCs can be differentiated into a wide range of cell types, allowing the generation of patient-specific cells suitable for cell-replacement therapy and disease modeling.

Despite this great promise, a number of studies suggest that reprogramming and the subsequent expansion of iPSCs in culture lead to the accumulation of diverse genetic abnormalities at chromosomal, subchromosomal, and nucleotide levels (Gore et al., 2011; Hussein et al., 2011; Laurent et al., 2011; Mayshar et al., 2010). The source of these genetic lesions remains under debate. Some reports attribute them primarily to clonal capture of variant cells within the donor cell population (Cheng et al., 2012; Young et al., 2012), yet another study suggests that approximately half of the mutations arise de novo during reprogramming (Gore et al., 2011). This has prompted us to examine the roles of the homologous recombination (HR) DNA repair pathway in reprogramming and whether reprogramming is a trigger of DNA damage.

We used a drug-inducible system to discriminate the effects of reprogramming from viral integration, because the latter is known to cause DNA double-strand breaks (DSBs). The results show that the ectopic expression of reprogramming factors is sufficient to induce DNA DSBs, providing a plausible molecular mechanism for genetic abnormalities observed in iPSC lines. Furthermore, efficient reprogramming requires key HR genes, including *Brca1*, *Brca2*, and *Rad51*, independently of the methods used to introduce reprogramming factors. Finally, deletion of the tumor suppressor *p53* largely restores normal reprogramming in HR-deficient mouse embryonic fibroblasts (MEFs), accompanied by a correction of reprogramming-dependent defects in cell proliferation and apoptosis. These findings provide important mechanistic insights into reprogramming and have important implications for designing rational approaches for the generation of lesion-free iPSCs suitable for clinical applications.

RESULTS

Reprogramming Induces DSBs

DNA DSBs can be triggered by a number of DNA-damaging agents, such as γ-irradiation and oxidative stress. Excessive

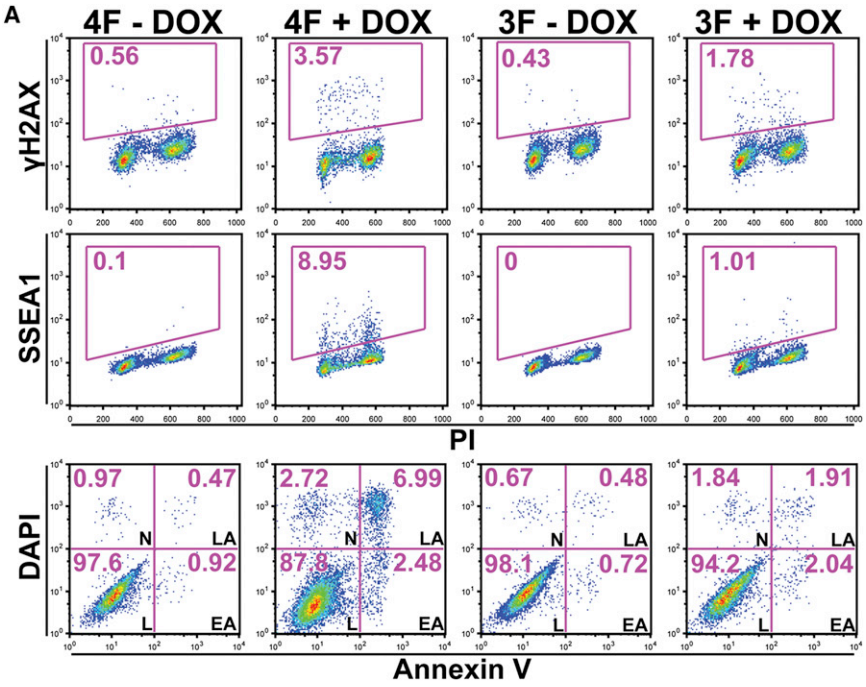

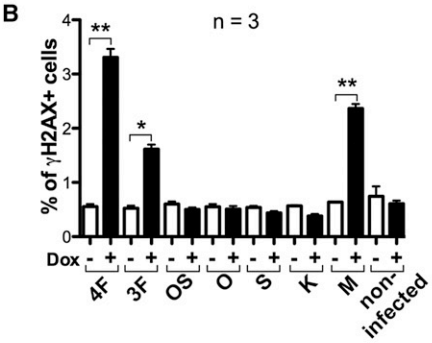

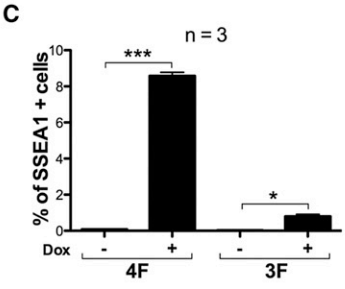

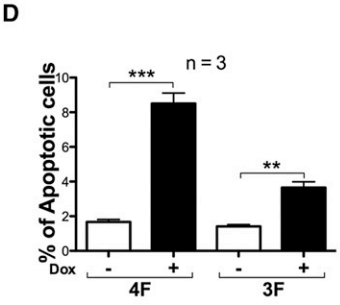

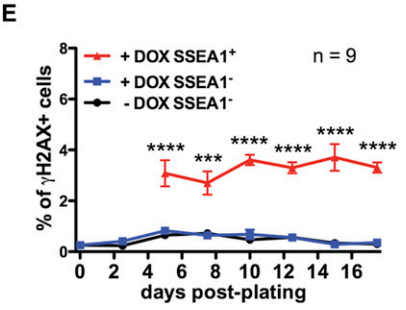

Figure 1. Reprogramming Induces DSBs and Apoptosis

(A) Representative fluorescence-activated cell sorting (FACS) plots of 4F- and 3F-infected wild-type MEFs stained for γH2AX, SSEA1, and Annexin V after cells were cultured with or without doxycycline (DOX) for 5 days. Numbers indicate percentages of positive cells. PI, propidium iodide; DAPI, 4'6-diamidino-2-phenylindole; L, alive; EA, early apoptotic; LA, late apoptotic; N, necrotic.

(B) Quantification of the percentage of γH2AX$^+$ cells in wild-type MEFs infected with reprogramming genes in combination or individually. OS, *Oct4-Sox2*; O, *Oct4*; S, *Sox2*; K, *Klf4*; M, *c-Myc*.

(C and D) Quantification of the percentage of SSEA1$^+$ (C) and Annexin V$^+$ (D) cells in wild-type MEFs transduced with 4F and 3F. Apoptotic cells are the sum of EA and LA cells.

(E) Time-lapse flow cytometric quantification of γH2AX$^+$ cells present in reprogrammable MEFs with or without DOX treatment; cells were separated based on expression of SSEA1. In all column graphs of this study, error bars indicate SEM and p values by two-tailed Student's t test. *, $p < 0.05$; **, $p < 0.01$; ***, $p < 0.001$; and ****, $p < 0.0001$, respectively.

accumulation of DSBs in a cell leads to growth arrest, apoptosis, or mutations in the genome. Ectopic expression of the reprogramming factors *Oct4*, *Sox2*, *Klf4*, and *c-Myc* or *Oct4*, *Sox2*, and *Klf4* (hereafter referred to as 4F or 3F, respectively) allows the reprogramming of MEFs to a pluripotent state (Hochedlinger and Plath, 2009; Okita and Yamanaka, 2011). Transduction of 4F or 3F with constitutive retroviral expression vectors has been shown to increase the number of cells with phosphorylated histone H2AX (γH2AX) nuclear foci, one of the earliest cellular responses to DSBs (Kawamura et al., 2009; Müller et al., 2012). However, it is unclear whether DSBs are caused by reprogramming or by viral transgene integration, given that the latter is known to cause DSBs (Skalka and Katz, 2005).

To determine whether there is a direct link between epigenetic reprogramming and increased DNA DSBs, we used doxycycline-inducible lentiviral vectors (FUW-tetO) to express reprogramming factors in wild-type (WT) MEFs and assessed γH2AX through flow cytometry (Huang and Darzynkiewicz, 2006). The effects of reprogramming genes were determined by comparing infected cells within the same pool with or without doxycycline treatment. We found that 4F- and 3F-infected MEFs showed a ~6-fold and a 3-fold increase, respectively, of γH2AX$^+$ cells after 5 days of doxycycline treatment in comparison to infected-but-untreated or noninfected MEFs, whereas doxycycline treatment alone on noninfected MEFs had no effect (Figures 1A and 1B). This correlated with the acquisition of an early reprogramming marker (SSEA1) and a marked increase in the percentage of cells undergoing apoptosis, as identified by Annexin V staining (Figures 1A, 1C, and 1D). Expressing *c-Myc* alone also had an effect, consistent with a previous report (Karlsson et al., 2003), whereas expressing other reprogramming factors individually or in combination (*Oct4* and *Sox2*) had no significant effect (Figure 1B).

Because nonintegrative methods are thought to generate safer iPSCs for clinical use, we measured γH2AX$^+$ cells during reprogramming using a nonintegrative approach that was based on the use of "reprogrammable" MEFs (Carey et al., 2010; Stadtfeld et al., 2010). We generated reprogrammable MEFs by combining an allele constitutively expressing the reverse tetracycline-controlled transactivator (rtTA) from the *Rosa26* locus with a doxycycline-inducible polycistronic reprogramming cassette (OKSM) targeted to the *Col1A1* locus (Stadtfeld et al., 2010). This system allows homogeneous expression of the reprogramming factors ideal for studies of reprogramming. Using flow cytometry, we analyzed the percentage of γH2AX$^+$ cells at different time points after doxycycline treatment. Additionally, we used the pluripotency cell surface marker SSEA1 to identify early reprogramming cells in doxycycline-treated conditions (Brambrink et al., 2008). We observed the same low levels of γH2AX expression in both untreated MEFs and SSEA1$^-$ cells in the doxycycline-treated condition (Figure 1E). In contrast, there was a significant increase in the percentage of γH2AX$^+$ cells in the SSEA1$^+$ population in doxycycline-treated cells. This increase occurred early and remained constant during the reprogramming process. These results demonstrate that reprogramming, rather than viral integration, is directly responsible for the accumulation of γH2AX in cells.

Reprogramming Is Impaired in *Brca1* and *Brca2* Mutant MEFs

In mammalian cells, three pathways have been described for the repair of DSBs: HR, nonhomologous end-joining (NHEJ), and single-strand annealing (SSA) (Moynahan and Jasin, 2010). HR is responsible for the accurate repair of DNA damage using the sister chromatid as a template. In contrast, repairs by NHEJ and SSA are intrinsically error-prone and can lead to deletions and other types of mutations. Previous studies have shown that fibroblasts defective for the Fanconi anemia (FA) complementation group are resistant to reprogramming through classic viral-infection-based methods (Müller et al., 2012; Raya et al., 2009). These studies suggest a potential link between HR and reprogramming, given that several FA pathway components have been shown to promote HR (Nakanishi et al., 2005). However, a direct role of HR in reprogramming has not been established because FA proteins also have distinct functions independent of HR.

We examined the role of *Brca1* and *Brca2*, two genes essential for homology-directed DNA repair, during reprogramming using homozygous MEFs generated from three hypomorphic mutant alleles. *Brca1*^{Tr} carries an insertion within exon 11, leading to a truncated Brca1 protein with 924 amino acids (Ludwig et al., 2001). The second *Brca1* allele, *Brca1*^{S1598F}, contains a point mutation in the Brca1 C-terminal domain which disrupts the interaction of Brca1 with the phosphorylated isoforms of several repair proteins including, Abraxas (CCDC98), BACH1 (FancJ), and CtIP (Shakya et al., 2011). The *Brca2*$^{\Delta 27}$ allele harbors a deletion of exon 27, which generates a truncated protein lacking 187 C-terminal amino acids (McAllister et al., 2002). All three mutations impair homology-directed DNA repair. Adult mice that are homozygous for each of these mutations are identified from crosses of heterozygous animals, suggesting that these mutations do not significantly affect cell growth or survival in vivo.

In WT MEFs, we typically detected ~300 alkaline phosphatase (AP)$^+$ colonies and ~100 Nanog$^+$ colonies 3 weeks after plating of 50,000 4F-infected cells using the constitutive retroviral expression vector pMXs (Figures 2A and 2B). In contrast, the numbers of AP$^+$ and Nanog$^+$ colonies were significantly reduced (up to ~20-fold) in *Brca1* and *Brca2* homozygous mutant MEFs when compared to WT control MEFs (Figures 2B–2D). By picking colonies with iPSC-like morphology, we were able to establish *Brca2* mutant iPSC lines with comparable efficiency (~40%) to WT controls (Figure S1A). *Brca2* mutant iPSCs were indistinguishable from control WT iPSCs in expression of *Nanog* and other pluripotency markers by real-time quantitative RT-PCR (qRT-PCR) and immunohistochemical analysis (Figure S1B and S1D). The rates of proliferation and apoptosis were not significantly different between *Brca2* mutant iPSC lines in comparison to control WT lines (Figures S1E–S1H). Therefore, the reprogramming phenotypes observed in *Brca2* mutant MEFs are not due to impaired proliferation and/or increased apoptosis of HR-deficient iPSCs formed during reprogramming. However, we were not able to establish a bona fide iPSC line from *Brca1* mutant MEFs out of the ten colonies picked (Figure S1A). The best *Brca1* mutant lines appeared partially reprogrammed, exhibiting only occasional Nanog staining by immunohistochemical analysis. In comparison to *Brca2* mutant and WT iPSC lines, *Brca1* mutant lines exhibited limited upregulation of the pluripotency gene *Nanog*, accompanied by incomplete silencing of the fibroblast marker *Col6a1* and reprogramming transgenes (Figures S1B–S1D). These data show that both *Brca1* and *Brca2* are required for efficient reprogramming, and that *Brca1* may also be required for iPSC-line establishment.

Next, we examined whether mutations in *Brca1* and *Brca2* affect 3F reprogramming without *c-Myc*, the overexpression of which alone increases DNA DBSs. Using doxycycline-inducible lentiviral expression vectors (FUW-tetO) to express 3F, we detected ~150 AP$^+$ colonies and ~40 Nanog$^+$ colonies 3 weeks after plating 50,000 infected, doxycycline-treated WT MEFs. As in 4F reprogramming, both *Brca1* and *Brca2* homozygous mutant MEFs showed up to a 20-fold reduction in the number of AP$^+$ colonies (Figures 2E and 2F). Moreover, no Nanog$^+$ colonies were detected (Figure 2G) from mutant MEFs. These results support a critical role of *Brca1* and *Brca2* in both 3F and 4F reprogramming independent of the infection method used to introduce reprogramming factors.

Finally, to establish a direct link between reprogramming and HR-mediated DNA repair, we compared the percentage of γH2AX$^+$ cells in *Brca1*$^{Tr/Tr}$ versus WT MEFs during reprogramming (Figure 2H). We detected a significant increase in the percentage of γH2AX$^+$ cells in both 4F- and 3F-expressing mutant cells in comparison to WT controls. These data, along with the established roles of *Brca1* and *Brca2* in HR, strongly suggest a direct involvement of HR-mediated DNA DSB repair in reprogramming.

HR Genes Play a Direct Role during Reprogramming

Brca1 and *Brca2* mutant MEFs may have accumulated genetic or cellular alterations during their culture before reprogramming,

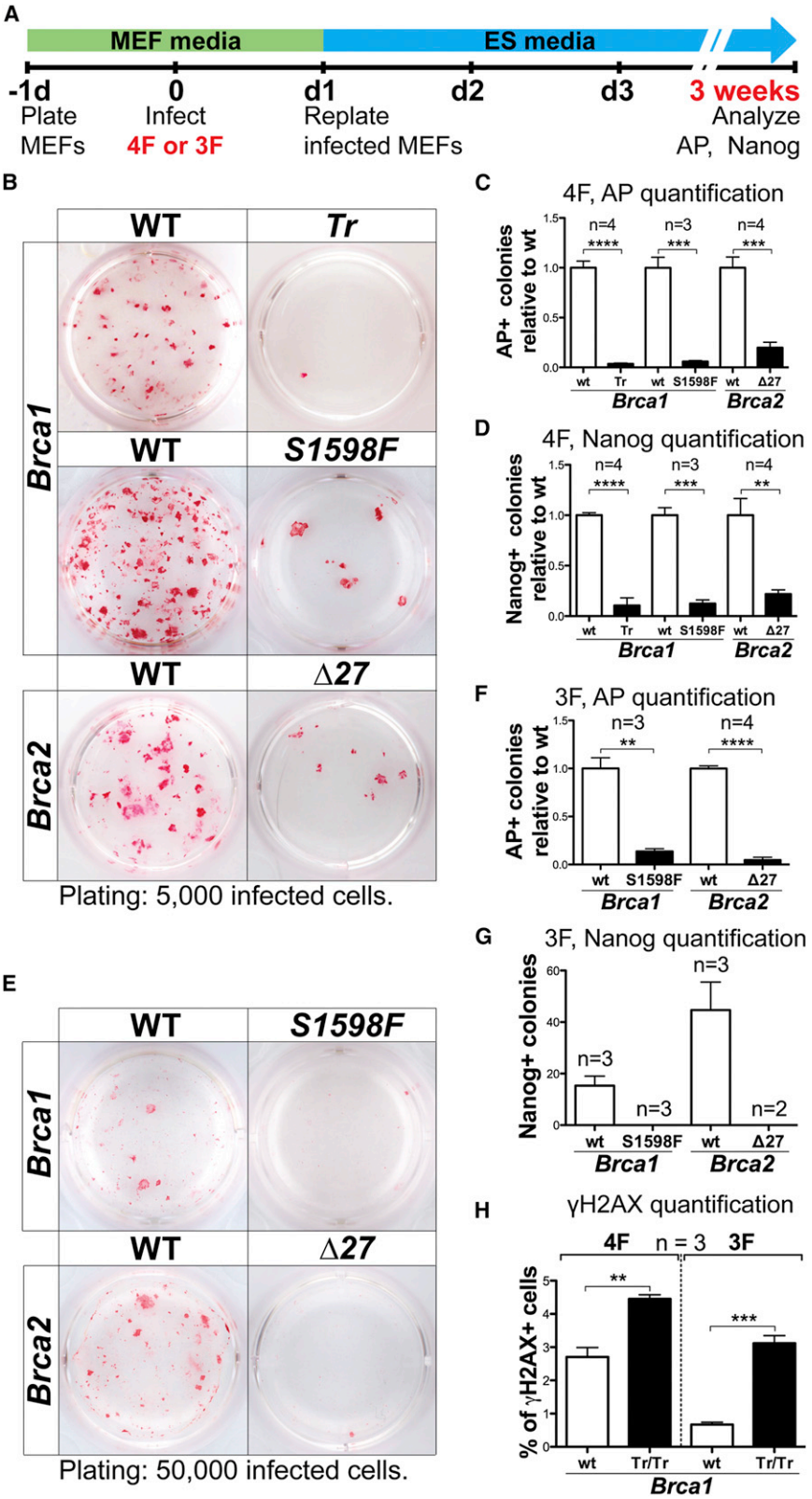

Figure 2. Reprogramming Is Impaired in *Brca1* and *Brca2* Mutant MEFs

(A) Schematics of all virus-mediated reprogramming experiments in this study. MEFs were infected with 4F or 3F 1 day after plating and replated in 12-well dishes the next day on irradiated MEFs at densities specified (indicated below the AP-staining pictures for all figures in this study). AP and Nanog staining was performed after 3 weeks (unless otherwise noted).

(B–D) Representative AP staining (B) and quantification of AP$^+$ (C) and Nanog$^+$ (D) colonies generated with 4F reprogramming from *Brca1*$^{Tr/Tr}$, *Brca1*$^{S1598F/S1598F}$, and *Brca2*$^{\Delta 27/\Delta 27}$ MEFs in comparison to wild-type (WT) MEFs from littermate controls.

(E–G) Representative AP staining (E) and quantification of AP$^+$ (F) and Nanog$^+$ (G) colonies generated with 3F reprogramming.

(H) Quantification of the percentage of γH2AX$^+$ cells in 4F- and 3F-infected, *Brca1*$^{Tr/Tr}$ mutant, and control wild-type MEFs after 5 days of DOX treatment.

See also Figure S1.

which could prevent the formation of iPSC colonies. Additionally, mutant MEFs show a small but significant decrease (<3% for FUW-tetO vectors) in gene-transduction efficiency in comparison to WT controls (Figures S2A and S2B), raising the possibility that mutant MEFs may reprogram less efficiently because of a requirement of HR genes for viral integration and transgene expression. To determine whether HR genes are directly required for reprogramming, we introduced 4F while simultaneously expressing small hairpin RNAs (shRNAs) against individual HR genes (*Brca1*, *Brca2*, and *Rad51*) in WT MEFs. Expectedly, knockdown of HR genes had no significant effect on the transduction of a GFP reporter or the reprogramming transgenes (Figures S2C and S2D). Significantly, a decrease in reprogramming efficiency was observed with all shRNAs except for one because of insufficient knockdown of the transcript (Figures 3A–3C and S3D). The most efficient shRNA (shRad51-b) reduced the number of AP^+ colonies by ~60-fold. Likewise, we performed shRNA-mediated knockdown of *Brca1*, *Brca2*, and *Rad51* in 3F reprogramming experiments and observed a marked decrease of AP^+ and $Nanog^+$ colonies (Figures S3A–S3C and S3E). Similar results were obtained with the use of an additional pluripotency marker gene, *Oct4*, by conducting reprogramming experiments on MEFs carrying one copy of the *Oct4-GFP* transgenic reporter allele (Szabó et al., 2002) (Figures 3D, 3E, S3F, and S3G).

The Requirement of HR Genes Is Independent of Viral Integration

The experiments described above introduced reprogramming genes with the use of classic viral-infection-based methods commonly used in reprogramming studies. However, viral integration triggers DNA DSBs (Skalka and Katz, 2005), which may necessitate HR-mediated DNA repair. Therefore, we proceeded to determine the requirement of HR genes in the absence of viral infection using reprogrammable MEFs. We infected reprogrammable MEFs with shRNAs targeting HR genes and added doxycycline to initiate reprogramming. Using a control shRNA, we detected, on average, ~600 alkaline AP^+ colonies (Figures 3D and 3F) and ~500 $Nanog^+$ colonies (Figure 3G) from 50,000 reprogrammable MEFs after ~3 weeks of doxycycline treatment. shRNAs against *Brca1*, *Brca2*, and *Rad51* all led to a marked decrease in the number of both AP^+ and $Nanog^+$ colonies (Figures 3D, 3F, 3G, and S3H). These results demonstrate that DNA damage increases during reprogramming independently of viral integration and that the HR pathway is also required for efficient reprogramming through nonintegrative methods.

p53 Deletion Rescues Reprogramming Defects of HR-Deficient MEFs

Because cells with excessive DNA damage are typically eliminated through p53-dependent apoptosis or growth arrest, we hypothesized that deletion of *p53* would rescue the reprogramming defects in HR-deficient MEFs. This would be consistent with an established role of the p53 pathway in limiting the rate of reprogramming (Spike and Wahl, 2011).

We performed 4F reprogramming on MEFs derived from *Brca2* homozygous mutant and WT embryos and used a well-characterized shRNA to simultaneously suppress *p53* (Hemann et al., 2003). Downregulating *p53* significantly increased reprogramming efficiency in both mutant and WT MEFs, though the reprogramming efficiency of mutant MEFs was not rescued to WT levels (Figures 4A–4C). This partial rescue may be due to incomplete inactivation of *p53* with the knockdown approach (Figure S4A). To further investigate the role of *p53* in HR-deficient MEFs, we generated $p53^{-/-}$ mutant MEFs (Jacks et al., 1994) and performed 4F reprogramming experiments while using shRNAs against *Brca1*, *Brca2*, and *Rad51*. In WT control MEFs, knockdown of HR genes caused a significant reduction in the number of AP^+ and $Nanog^+$ colonies (Figures 4D–4F and S4B). A ~20-fold increase in the numbers of AP^+ and $Nanog^+$ colonies was observed in $p53^{-/-}$ mutant MEFs in comparison to WT control MEFs, consistent with previous reports. However, knockdown of HR genes generally had no significant effect on the reprogramming of $p53^{-/-}$ mutant MEFs (Figures 4D–4F).

To further investigate the cellular mechanisms, we analyzed cell proliferation and apoptosis during reprogramming by immunostaining for the mitotic marker phospho-Histone H3 and the apoptotic marker cleaved Caspase-3. During 4F reprogramming of WT control MEFs, HR deficiency caused a significant decrease in the percentage of proliferating cells and an increase of apoptotic cells (Figures 4G, 4H, S4C, and S4D). In contrast, during 4F reprogramming of $p53^{-/-}$ MEFs, HR deficiency failed to cause any significant defects in cell proliferation or apoptosis (some increase was observed in apoptosis, though it was not statistically significant) (Figures 4G, 4H, S4C, and S4D). These results suggest that a defective HR pathway leads to an increased number of cells accumulating DNA damage during reprogramming. p53-mediated growth arrest and apoptosis is responsible for the elimination of these cells and, consequently, a significant decrease in reprogramming efficiency. Although downregulating *p53* rescues the reprogramming phenotype in HR-deficient MEFs, it may also allow the generation of iPSCs with genetic aberrations (Figure 4I).

DISCUSSION

Current reprogramming strategies rely on the ectopic expression of defined sets of pluripotency-associated transcription factors (Hochedlinger and Plath, 2009; Okita and Yamanaka, 2011). The recent development of nonintegrative methods for introducing reprogramming genes theoretically circumvents undesirable genetic modifications in iPSCs caused by transgene insertions in classic reprogramming approaches (González et al., 2011). However, surveys of iPSCs generated with both integrative and nonintegrative methods reveal significant genetic abnormalities (Gore et al., 2011; Hussein et al., 2011; Laurent et al., 2011; Mayshar et al., 2010). Here, we show that ectopic expression of reprogramming factors increases the level of the DNA DSB marker γH2AX independently of viral integration. This effect may be linked to oncogenic activities of reprogramming factors (Daley, 2008). On the other hand, epigenetic remodeling, including global DNA demethylation, may also contribute to DNA damage during reprogramming. Although the mechanisms by which 5-methylcytosine is converted into cytosine in CpG islands are not yet well understood, prevailing models suggest that this conversion involves potentially mutagenic

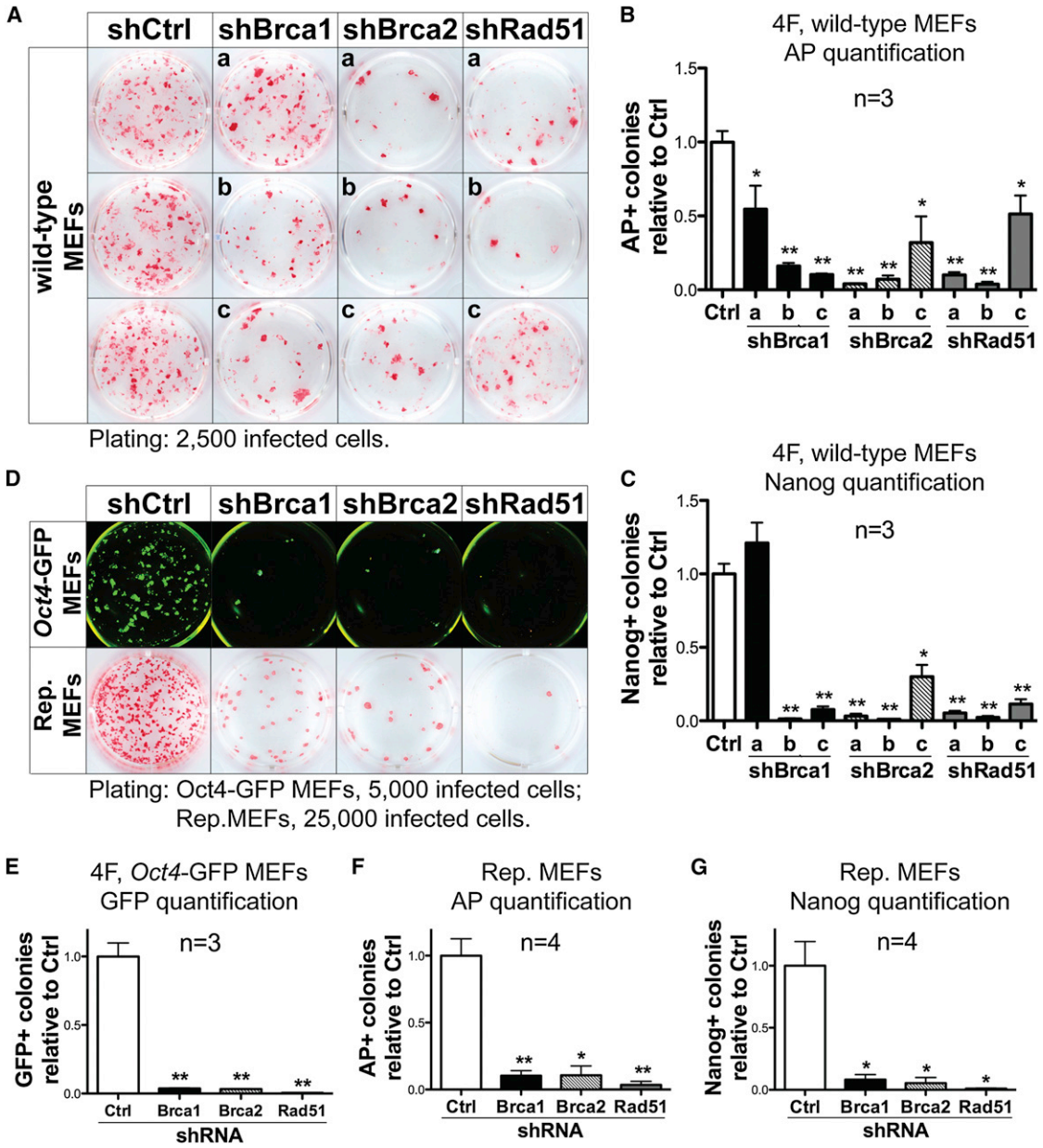

Figure 3. HR Genes Are Directly Required during Reprogramming

(A–C) Representative AP staining (A) and quantification of AP$^+$ (B) and Nanog$^+$ (C) colonies generated with 4F reprogramming and a panel of shRNAs targeting *Brca1* (shBrca1-a, shBrca1-b, and shBrca1-c), *Brca2* (shBrca1-a, shBrca1-b, and shBrca1-c), and *Rad51* (shRad51-a, shRad51-b, and shRad51-c) compared to the shRNA control vector (shCtrl). Lower case letters refer to individual shRNAs targeting each HR gene. shBrca1-c, shBrca2-b, and shRad51-b were used for further experiments.

(D) The upper panel shows representative fluorescence images of *Oct4*-GFP$^+$ colonies generated with 4F and shRNAs targeting HR genes. The lower panel shows representative AP staining images from reprogrammable (Rep.) MEFs infected with shRNAs against HR genes.

(E) Quantification of *Oct4*-GFP$^+$ colonies from experiments with 4F-infected *Oct4*-GFP MEFs and acute HR-gene knockdown.

(F and G) Quantification of AP$^+$ (F) and Nanog$^+$ (G) colonies from experiments using reprogrammable MEFs and acute HR-gene knockdown.

See also Figures S2 and S3.

DNA modifications that need to be processed through DNA repair mechanisms (Teperek-Tkacz et al., 2011).

Our results show that an intact HR pathway is required for efficient reprogramming, even in the absence of viral integration or potential genome-modifying agents, such as the oncogene *c-Myc*. The complete loss of function of HR genes during reprogramming may lead to even more profound effects. HR genes may also have functions in addition to DNA repair during reprogramming. For example, Brca1 is implicated in basal transcriptional regulation (Mullan et al., 2006) and transcriptional

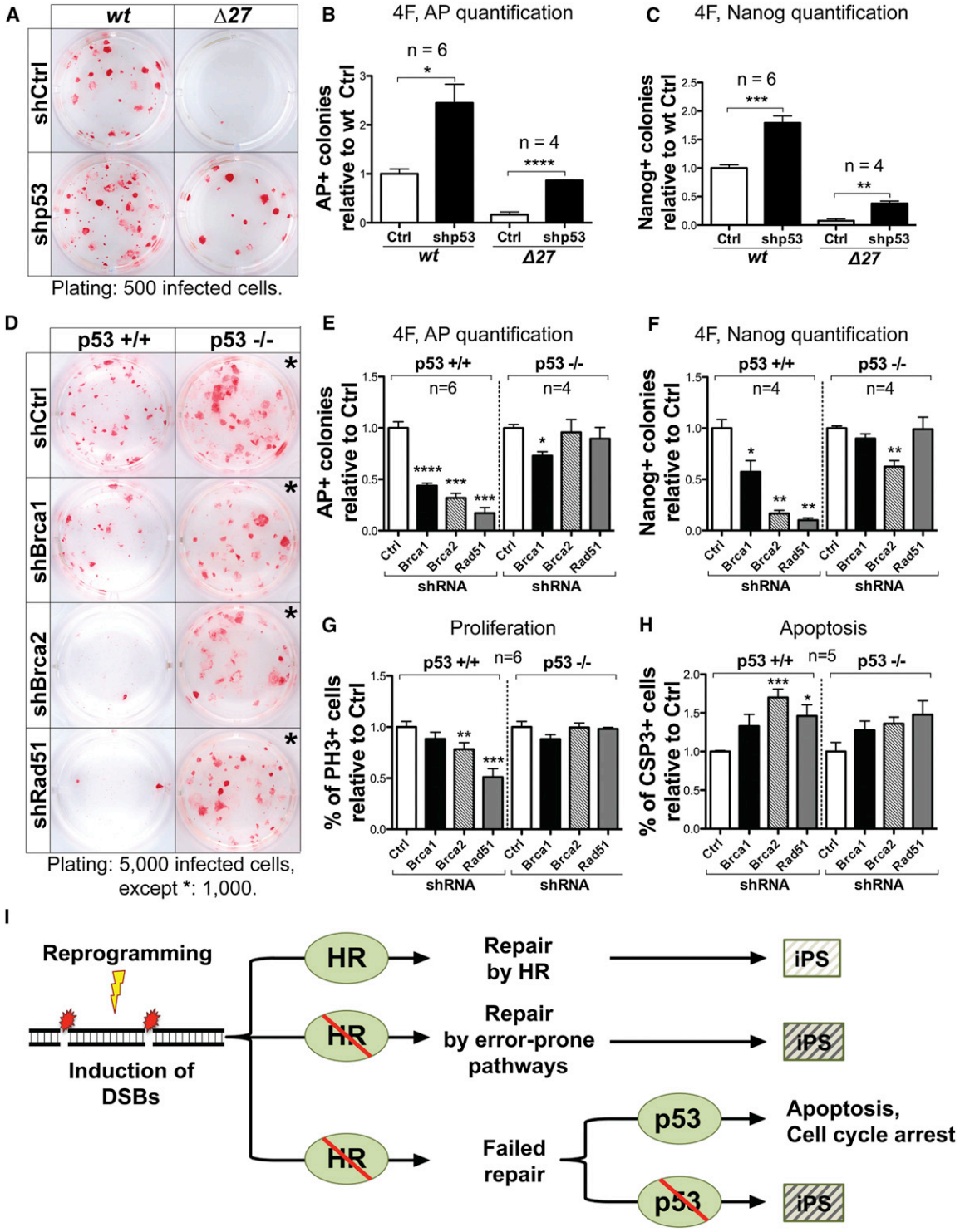

Figure 4. Downregulating *p53* Rescues the Reprogramming Phenotype of HR-Defective MEFs

(A–C) Representative AP staining (A) and quantification of AP$^+$ (B) and Nanog$^+$ (C) colonies generated with 4F reprogramming from *Brca2*$^{\Delta 27}$ homozygous mutant and wild-type MEFs infected with an shRNA targeting p53 (shp53) or vector control (shCtrl).

(D–F) Representative AP staining (D) and quantification of AP$^+$ (E) and Nanog$^+$ (F) colonies generated with 4F reprogramming from *p53*$^{-/-}$ and wild-type MEFs under acute HR-gene knockdown. All staining were performed 16 days after infected cells were replated.

(G and H) Quantification of the percentage of Phospho-Histone H3$^+$ (PH3$^+$) (G) and Cleaved Caspase-3$^+$ (CSP3$^+$) (H) cells 6 days postinfection of 4F and HR gene knockdown in *p53*$^{-/-}$ mutant and wild-type MEFs.

(legend continued on next page)

activation of several genes, including *Sox2* (Kondo and Raff, 2004). These additional roles may explain the stronger reprogramming phenotype observed in *Brca1* mutant MEFs in comparison to *Brca2* mutant cells. However, differences in genetic background and/or severity of the hypomorphic alleles used in this work may have also contributed to the phenotypic differences. Recent evidence that core components of the nucleotide excision repair pathway act as ESC-specific transcriptional coactivators regulating the expression of *Nanog* (Fong et al., 2011) raises the interesting possibility that additional DNA repair pathway components may also be co-opted in ESCs to maintain pluripotency.

Finally, a better understanding of the role of DNA repair pathways during reprogramming will contribute to the identification of safer approaches for creating iPSCs. The generation of desired cell types for regenerative medicine can also be achieved with the use of more direct approaches, such as lineage reprogramming. When compared to pluripotency reprogramming, lineage reprogramming may involve less extensive epigenetic remodeling, and it does not typically rely on ectopic expression of classic oncogenes. For regenerative medicine, it will be crucial to determine whether lineage reprogramming induces levels of DNA damage similar to pluripotency reprogramming and to assess its mutagenic impact.

EXPERIMENTAL PROCEDURES

Mouse Strains

All animal experiments are approved by Institutional Animal Care and Use Committee (IACUC) of Memorial Sloan-Kettering Cancer Center.

Reprogramming and Generation of iPSC Lines

For reprogramming experiments, passage 2 MEFs were seeded at 2×10^5 cells per well of a 6-well dish. MEFs were infected twice on the next day with fresh viral supernatants. The day after infection, MEFs were replated at different specified densities on irradiated MEF feeder layers and cultured in mouse ESC media (knockout DMEM supplemented with 15% Hyclone FBS, L-glutamine, penicillin and streptomycin, nonessential amino acids, β-mercaptoethanol, and 1000 U/ml leukemia inhibitory factor). See Extended Experimental Procedures for a detailed description of the reprogramming experiments performed in this article.

Knockdown of Gene Expression with shRNAs

To knock down expression of *Brca1*, *Brca2*, and *Rad51* genes, we obtained pLKO.1-puro lentiviral vectors expressing three different shRNAs per gene from Sigma-Aldrich (MISSION shRNA constructs). In all experiments, knockdown efficiency was assessed by qRT-PCR analyses 6 days after infection and compared to the expression of the corresponding gene in cells infected with an empty pLKO.1-puro control virus (Sigma-Aldrich, SHC001) (Figures S3D, S3E, S3G, S3H, and S4B). We used a well-characterized shRNA (MLS-shp53) (Hemann et al., 2003) to knock down p53 expression and used the empty vector (MLS-empty) as a control (Figure S4A).

Alkaline Phosphatase and Immunofluorescence Staining

Alkaline phosphatase (AP) staining was performed with the use of a Vector Red Alkaline Phosphatase Substrate Kit according to the manufacturer's guidelines (Vector Laboratories, SK-5100). For nuclear immunostaining, cells were fixed with 4% paraformaldehyde in PBS for ~10 min and stained by standard immunofluorescence staining procedures. The following primary antibodies were used: Nanog (Cosmo Bio, REC-RCAB0002P-F), Oct4 (Santa Cruz Biotechnology, sc-5279), Klf4 (Santa Cruz Biotechnology, sc-20691), and Sox2 (Santa Cruz Biotechnology, sc-17320). For SSEA1 surface marker expression analysis, live cells were directly stained for 30 min with an SSEA1 antibody conjugated with Alexa 488 (Santa Cruz Biotechnology, sc-21702 AF488) in PBS with 0.2% BSA.

Proliferation and Apoptosis Immunofluorescence Analysis

For proliferation and apoptosis analyses, cells (infected on the previous day, or not infected) were plated at 10^4 cells per well of a 48-well dish. Five days after plating, cells were fixed with 4% paraformaldehyde in PBS for ~10 min. Immunofluorescence staining with the use of either a Phospho-Histone H3 (Ser10) antibody (PH3) (Cell Signaling Technology, 9701S) or a Cleaved Caspase-3 (Asp175) antibody (CSP3) (Cell Signaling Technology, 9661S) was performed according to standard procedures. In both cases, detection was achieved with the use of a donkey anti-rabbit Alexa 488 secondary antibody (Life Technologies, A21206) combined with DAPI nuclear staining. Plates were imaged in multiple fluorescence channels with the use of a Cellomics ArrayScan HCS Reader (Thermo Scientific) (PH3: Objective 10×, channel 1 dye XF53_386_23, channel 2 dye XF53_485_20; CSP3: Objective 10×, channel 1 dye BGRFR_386_23, channel 2 dye XF53_485_20). Automated image analysis of $PH3^+$ cells (nuclear staining) was performed with the use of Target Activation BioApplication V4, whereas quantification of $CSP3^+$ cells (cytoplasmic staining) was performed with the use of Compartmental AnalysisV4 (Figures S4C and S4D).

Flow Cytometric Analysis of γH2AX and SSEA1

Cells were first incubated with the SSEA1 antibody conjugated with Alexa 488 (described above) for 30 min. After the washing steps, cells were fixed in 70% ice cold ethanol and stored at −20°C for up to 2 weeks. Next, cells were incubated with a phospho-Histone H2A.X (Ser139) antibody (Millipore, 05-636) followed by the Alexa 647 goat anti-mouse IgG1 secondary antibody (Life Technologies, A21240) for γH2AX detection. Finally, cells were stained with propidium iodide (PI) solution (PBS containing 5 μg/ml PI and 100 μg/ml RNase A) prior to flow cytometric analysis with a Becton Dickinson FACSCalibur.

Flow Cytometric Analysis of Annexin V and SSEA1

For apoptosis assays, flow cytometry was performed on cells stained with Annexin V–FITC (BD Pharmingen, 556547) and DAPI. In some experiments, cells were also stained with SSEA1-APC (R&D Systems, FAB2155A). In brief, cells were washed twice with PBS and stained with 0.5 μl of Annexin V–FITC (or with 0.5 μl of Annexin V-FITC and 4 ul SSEA1-APC) in 100 μl binding buffer (10 mM HEPES, [pH 7.4], 140 mM NaOH, 2.5 mM CaCl2) for 30 min at room temperature in the dark. Next, cells were washed twice with the binding buffer and then resuspended in a binding buffer containing 1 μg/ml DAPI. Apoptotic cells were detected with a Beckman Coulter CyAn ADP Analyzer. Both early apoptotic ($Annexin\ V^+$, $DAPI^-$) and late apoptotic ($Annexin\ V^+$, $DAPI^+$) cells were included in cell death quantifications.

Statistical Analysis

All values are shown as mean ± SEM. p values were calculated with the use of a two-tailed Student's t test; $p < 0.05$ (*) was considered significant.

SUPPLEMENTAL INFORMATION

Supplemental Information includes Extended Experimental Procedures, four figures, and two tables and can be found with this article online at http://dx.doi.org/10.1016/j.celrep.2013.02.005.

(I) Our results support a critical role of the HR pathway for efficient reprogramming. We propose a model in which reprogramming increases the level of DNA damage, which is responsible for the genetic aberrations observed in iPSC lines (indicated by a lightly shaded box). A defective HR pathway may lead to increased genetic aberration (indicated by dark shaded boxes) or the elimination of abnormal cells through p53-mediated cell-cycle arrest or apoptosis. See also Figure S4.

LICENSING INFORMATION

This is an open-access article distributed under the terms of the Creative Commons Attribution-NonCommercial-No Derivative Works License, which permits non-commercial use, distribution, and reproduction in any medium, provided the original author and source are credited.

ACKNOWLEDGMENTS

We thank Shinya Yamanaka, Rudolf Jaenisch, Didier Trono, and Bob Weinberg for providing viral expression and packaging vectors through Addgene; Wenjun Guo for the FUW-tetO vector; Hans-Guido Wendel and Elisa Oricchio for p53 shRNA constructs; Kathryn Anderson, Hisham Bazzi, and Raymond Wang for providing mutant mice for MEF isolation; Zengrong Zhu, Katia Manova-Todorova, and Sanghoon Oh for assisting with image acquisition and analysis; Diane Domingo and Jennifer Wilshire for assistance with flow cytometry; and members of the Huangfu and Jasin laboratories, Mark Tomishima, and Wenjun Guo for critical reading of the manuscript. This study was funded in part by the Louis V. Gerstner Jr. Young Investigators Award and Memorial Sloan-Kettering Cancer Center Society Special Projects Committee. F.G. was supported by the New York State Stem Cell Science fellowship from the Center for Stem Cell Biology of the Sloan-Kettering Institute. F.V. was supported by an American-Italian Cancer Foundation Postdoctoral Research Fellowship.

Received: October 31, 2012
Revised: January 15, 2013
Accepted: February 4, 2013
Published: March 7, 2013

REFERENCES

Brambrink, T., Foreman, R., Welstead, G.G., Lengner, C.J., Wernig, M., Suh, H., and Jaenisch, R. (2008). Sequential expression of pluripotency markers during direct reprogramming of mouse somatic cells. Cell Stem Cell *2*, 151–159.

Carey, B.W., Markoulaki, S., Beard, C., Hanna, J., and Jaenisch, R. (2010). Single-gene transgenic mouse strains for reprogramming adult somatic cells. Nat. Methods *7*, 56–59.

Cheng, L., Hansen, N.F., Zhao, L., Du, Y., Zou, C., Donovan, F.X., Chou, B.K., Zhou, G., Li, S., Dowey, S.N., et al.; NISC Comparative Sequencing Program. (2012). Low incidence of DNA sequence variation in human induced pluripotent stem cells generated by nonintegrating plasmid expression. Cell Stem Cell *10*, 337–344.

Daley, G.Q. (2008). Common themes of dedifferentiation in somatic cell reprogramming and cancer. Cold Spring Harb. Symp. Quant. Biol. *73*, 171–174.

Fong, Y.W., Inouye, C., Yamaguchi, T., Cattoglio, C., Grubisic, I., and Tjian, R. (2011). A DNA repair complex functions as an Oct4/Sox2 coactivator in embryonic stem cells. Cell *147*, 120–131.

González, F., Boué, S., and Izpisúa Belmonte, J.C. (2011). Methods for making induced pluripotent stem cells: reprogramming à la carte. Nat. Rev. Genet. *12*, 231–242.

Gore, A., Li, Z., Fung, H.L., Young, J.E., Agarwal, S., Antosiewicz-Bourget, J., Canto, I., Giorgetti, A., Israel, M.A., Kiskinis, E., et al. (2011). Somatic coding mutations in human induced pluripotent stem cells. Nature *471*, 63–67.

Hemann, M.T., Fridman, J.S., Zilfou, J.T., Hernando, E., Paddison, P.J., Cordon-Cardo, C., Hannon, G.J., and Lowe, S.W. (2003). An epi-allelic series of p53 hypomorphs created by stable RNAi produces distinct tumor phenotypes in vivo. Nat. Genet. *33*, 396–400.

Hochedlinger, K., and Plath, K. (2009). Epigenetic reprogramming and induced pluripotency. Development *136*, 509–523.

Huang, X., and Darzynkiewicz, Z. (2006). Cytometric assessment of histone H2AX phosphorylation: a reporter of DNA damage. Methods Mol. Biol. *314*, 73–80.

Hussein, S.M., Batada, N.N., Vuoristo, S., Ching, R.W., Autio, R., Närvä, E., Ng, S., Sourour, M., Hämäläinen, R., Olsson, C., et al. (2011). Copy number variation and selection during reprogramming to pluripotency. Nature *471*, 58–62.

Jacks, T., Remington, L., Williams, B.O., Schmitt, E.M., Halachmi, S., Bronson, R.T., and Weinberg, R.A. (1994). Tumor spectrum analysis in p53-mutant mice. Curr. Biol. *4*, 1–7.

Karlsson, A., Deb-Basu, D., Cherry, A., Turner, S., Ford, J., and Felsher, D.W. (2003). Defective double-strand DNA break repair and chromosomal translocations by MYC overexpression. Proc. Natl. Acad. Sci. USA *100*, 9974–9979.

Kawamura, T., Suzuki, J., Wang, Y.V., Menendez, S., Morera, L.B., Raya, A., Wahl, G.M., and Izpisúa Belmonte, J.C. (2009). Linking the p53 tumour suppressor pathway to somatic cell reprogramming. Nature *460*, 1140–1144.

Kondo, T., and Raff, M. (2004). Chromatin remodeling and histone modification in the conversion of oligodendrocyte precursors to neural stem cells. Genes Dev. *18*, 2963–2972.

Laurent, L.C., Ulitsky, I., Slavin, I., Tran, H., Schork, A., Morey, R., Lynch, C., Harness, J.V., Lee, S., Barrero, M.J., et al. (2011). Dynamic changes in the copy number of pluripotency and cell proliferation genes in human ESCs and iPSCs during reprogramming and time in culture. Cell Stem Cell *8*, 106–118.

Ludwig, T., Fisher, P., Ganesan, S., and Efstratiadis, A. (2001). Tumorigenesis in mice carrying a truncating Brca1 mutation. Genes Dev. *15*, 1188–1193.

Mayshar, Y., Ben-David, U., Lavon, N., Biancotti, J.C., Yakir, B., Clark, A.T., Plath, K., Lowry, W.E., and Benvenisty, N. (2010). Identification and classification of chromosomal aberrations in human induced pluripotent stem cells. Cell Stem Cell *7*, 521–531.

McAllister, K.A., Bennett, L.M., Houle, C.D., Ward, T., Malphurs, J., Collins, N.K., Cachafeiro, C., Haseman, J., Goulding, E.H., Bunch, D., et al. (2002). Cancer susceptibility of mice with a homozygous deletion in the COOH-terminal domain of the Brca2 gene. Cancer Res. *62*, 990–994.

Moynahan, M.E., and Jasin, M. (2010). Mitotic homologous recombination maintains genomic stability and suppresses tumorigenesis. Nat. Rev. Mol. Cell Biol. *11*, 196–207.

Mullan, P.B., Quinn, J.E., and Harkin, D.P. (2006). The role of BRCA1 in transcriptional regulation and cell cycle control. Oncogene *25*, 5854–5863.

Müller, L.U., Milsom, M.D., Harris, C.E., Vyas, R., Brumme, K.M., Parmar, K., Moreau, L.A., Schambach, A., Park, I.H., London, W.B., et al. (2012). Overcoming reprogramming resistance of Fanconi anemia cells. Blood *119*, 5449–5457.

Nakanishi, K., Yang, Y.G., Pierce, A.J., Taniguchi, T., Digweed, M., D'Andrea, A.D., Wang, Z.Q., and Jasin, M. (2005). Human Fanconi anemia monoubiquitination pathway promotes homologous DNA repair. Proc. Natl. Acad. Sci. USA *102*, 1110–1115.

Okita, K., and Yamanaka, S. (2011). Induced pluripotent stem cells: opportunities and challenges. Philos. Trans. R. Soc. Lond. B Biol. Sci. *366*, 2198–2207.

Raya, A., Rodríguez-Pizà, I., Guenechea, G., Vassena, R., Navarro, S., Barrero, M.J., Consiglio, A., Castellà, M., Río, P., Sleep, E., et al. (2009). Disease-corrected haematopoietic progenitors from Fanconi anaemia induced pluripotent stem cells. Nature *460*, 53–59.

Shakya, R., Reid, L.J., Reczek, C.R., Cole, F., Egli, D., Lin, C.S., deRooij, D.G., Hirsch, S., Ravi, K., Hicks, J.B., et al. (2011). BRCA1 tumor suppression depends on BRCT phosphoprotein binding, but not its E3 ligase activity. Science *334*, 525–528.

Skalka, A.M., and Katz, R.A. (2005). Retroviral DNA integration and the DNA damage response. Cell Death Differ. *12*(*Suppl 1*), 971–978.

Spike, B.T., and Wahl, G.M. (2011). p53, Stem Cells, and Reprogramming: Tumor Suppression beyond Guarding the Genome. Genes Cancer *2*, 404–419.

Stadtfeld, M., Maherali, N., Borkent, M., and Hochedlinger, K. (2010). A reprogrammable mouse strain from gene-targeted embryonic stem cells. Nat. Methods *7*, 53–55.

Szabó, P.E., Hübner, K., Schöler, H., and Mann, J.R. (2002). Allele-specific expression of imprinted genes in mouse migratory primordial germ cells. Mech. Dev. *115*, 157–160.

Takahashi, K., and Yamanaka, S. (2006). Induction of pluripotent stem cells from mouse embryonic and adult fibroblast cultures by defined factors. Cell *126*, 663–676.

Teperek-Tkacz, M., Pasque, V., Gentsch, G., and Ferguson-Smith, A.C. (2011). Epigenetic reprogramming: is deamination key to active DNA demethylation? Reproduction *142*, 621–632.

Young, M.A., Larson, D.E., Sun, C.W., George, D.R., Ding, L., Miller, C.A., Lin, L., Pawlik, K.M., Chen, K., Fan, X., et al. (2012). Background mutations in parental cells account for most of the genetic heterogeneity of induced pluripotent stem cells. Cell Stem Cell *10*, 570–582.